POAC'25
St. John's, Newfoundland and Labrador, Canada

Proceedings of the 28th International Conference on Port and Ocean Engineering under Arctic Conditions
Jul 13-17, 2025
St. John's, Newfoundland and Labrador
Canada

Effect of ice drift parameters to estimated fatigue damage in an offshore wind foundation

Eeva Mikkola[1], Jaakko Heinonen[1], Maria Tikanmäki[1,2]

[1] VTT, Espoo, Finland

[2] Lapland University of Applied Sciences, Rovaniemi, Finland

ABSTRACT

In the Bothnian Bay, sea ice is present multiple months each winter and ice loads from drifting ice need to be considered in fatigue design of offshore wind turbines. For defining the ice loads, ice thickness together with ice drift speed and direction are required. Ice thicknesses have been reported in ice charts for many decades, whereas ice drift speed and direction are typically calculated from wind data. The aim of this study is to quantify the sensitivity of offshore wind turbine fatigue analysis to these input ice conditions. 42 years of ice chart and ERA5 wind data were used to estimate the relevant loading scenarios and their frequency for the wind turbine lifetime for a site in the Bay of Bothnia. Resulting stress histories and fatigue damage from 25 ice seasons were simulated for one location in the foundation. The simulated structure is the IEA 15 MW reference wind turbine with a monopile foundation and an ice breaking cone. The results showed that changes in input ice drift parameters can double the calculated fatigue damage for ice load events. In the simulations, as the ice load peaks occur relatively infrequently in comparison to wind load peaks, the timing of these load peaks in relation to each other becomes a significant factor defining the highest stress ranges from the loading history.

KEY WORDS Offshore wind; Foundations; Fatigue; Ice conditions; Ice loads

INTRODUCTION

In the Baltic Sea, structural design of offshore wind turbines needs to account for ice loads. In the southern Baltic Sea sea ice occurs only periodically and conventional wind turbine foundation design is applicable. In the Bay of Bothnia, in the northern Baltic Sea, sea ice is present for many months every winter with regular events of drifting ice and presence of ice ridges (example of typical ice conditions shown in Figure 1). For this area, an ice-breaking cone at water level is proposed as the most viable structural solution for mitigating ice loads. Having an inclined surface changes the ice failure mode from crushing to bending, thus reducing the ice loads. The drawback is that with the cone the addition of material - steel and concrete - can be around 30% of the total weight of the structure. This means that knowing the ice conditions during the lifetime of the structure is crucial for reliable and cost-effective structural design, including the choice of cone dimensions.

For fatigue design it is crucial that all relevant dynamic load events during the lifetime of the structure are accounted for as fatigue damage accumulates slowly and from load levels relatively small when compared to the ultimate loads experienced by the structure. IEC 61400-

3 (2019) standard states that for assessing dynamic ice load effects on offshore wind turbines and whether frequency lock-in or resonant vibration happens, ice mobility, floe sizes, ice concentration, ice types and misalignment between wind and ice drift directions should be considered. From the turbine point of view, both power production and parked condition need to be accounted for. For fatigue analysis, all relevant ice thicknesses, ice drift speeds and ice drift directions together with their duration are needed. For the Bay of Bothnia, ice thicknesses are available from the Finnish-Swedish ice charts, but ice drift speeds and directions are available only from dedicated measuring campaigns or from simulations of sea ice dynamics. Further south, the infrequency of ice makes the choices of a relevant ice thickness distribution as well as the ice drift distribution challenging. Hornnes et al. (2022) have looked at the use of Copernicus reanalysis data to define relevant ice thicknesses for fatigue damage calculation for Kriegers Flak in southern Baltic Sea, whereas Tikanmäki and Heinonen (2021) looked at maximum level ice and ice ridge consolidated layer thicknesses in the same area. Braun et al. (2022) constructed a full load spectra including wind, wave and ice loads for an offshore structure located in Southern Baltic Sea, but did not conclude on the fatigue damage contribution of the ice loads.

In the Bay of Bothnia, sea ice movement is mostly driven by wind due to lack of strong currents. In this area, according to Leppäranta (2011), the wind driven ice drift speed is on average 2-3% of the wind speed at 10 m height from the water surface and the drift direction is 30° right from the wind direction due to Coriolis force. Accordingly, DNVGL-ST-0437 standard (2016) proposes to use ice drift speeds of 2.5% of wind speeds at 10 m height. In reality, ice floe drift speed is affected by other factors as well, including ice concentration in the area and the floe size itself. For free drift, the ice drift direction is close to the wind direction. For higher ice concentration, different values up to 20° misalignment between wind and ice direction have been proposed (Sinsabvarodom, et al., 2022, Leppäranta, 2011). In the Bay of Bothnia, both the fast ice edge and other ice floes restrict free drift. This shows in measurement campaigns as large variation in the ice drift speeds and directions in relation to wind.

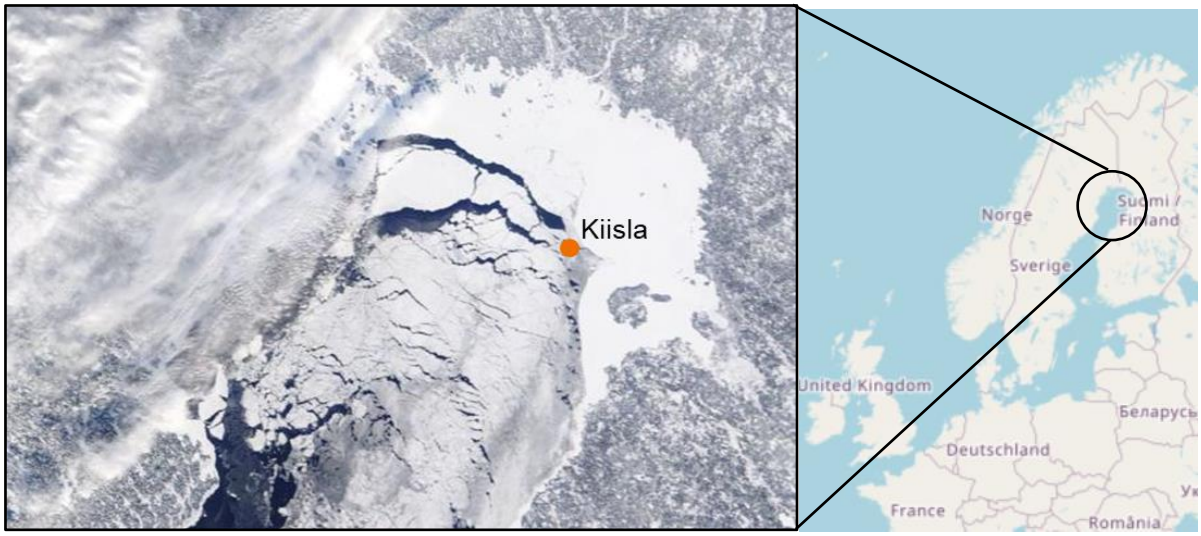

Figure 1. Kiisla area in the Bay of Bothnian, NASA Terra MODIS satellite image from 25.2.2023. Black is open water, white is ice. Kiisla location in drifting ice zone close to fast ice edge. Map data from OpenStreetMap.

METHODS

Structural model

The structural model is based on the IEA 15 MW reference offshore wind turbine (Gaertner et al., 2020) fitted with an ice-breaking cone at the water level – see Figure 2. Tower diameter is 10 m at tower start (15 m above water level) and 6.5 m at tower top. Foundation diameter is 11 m. The ice breaking cone height is 2 m above water level and 2.5 m below water level with a cone angle of 60° and friction coefficient of 0.1 between the structure and ice. Here, the turbine and the cone are modelled as dead masses (turbine 1 017 tons and cone 987 tons) and the tower and foundation are modelled with 195 linear thin-walled pipe elements with 6 degrees of freedom. The soil-structure interaction at seabed is modelled with soil springs according to a simplified spring model introduced in the standard NCCI 7 Eurokoodin soveltamisohje (2017). Seabed was considered to be frictional and non-cohesive soil with material properties based on seabed measurements provided by Ponvia.

The wind loads consist of a concentrated thrust load for the turbine and a distributed line load for the tower, both using a normal turbulence model. Structural damping is 1%, whereas different aerodynamic damping parameters are used depending on the operational status. For idling the aerodynamic damping is omitted. For operation, the damping ranges from 0.5% for hub wind speed of 3.6 m/s to 3.5% for hub wind speed of 25.4 m/s. Ice loads from drifting level ice consist of concentrated vertical and horizontal loads. The wind and ice loads are given as 10-minute time histories, where the ice and wind load histories are independent of each other. Wave loads are not considered as the analysis includes only periods with ice cover, when there are no waves.

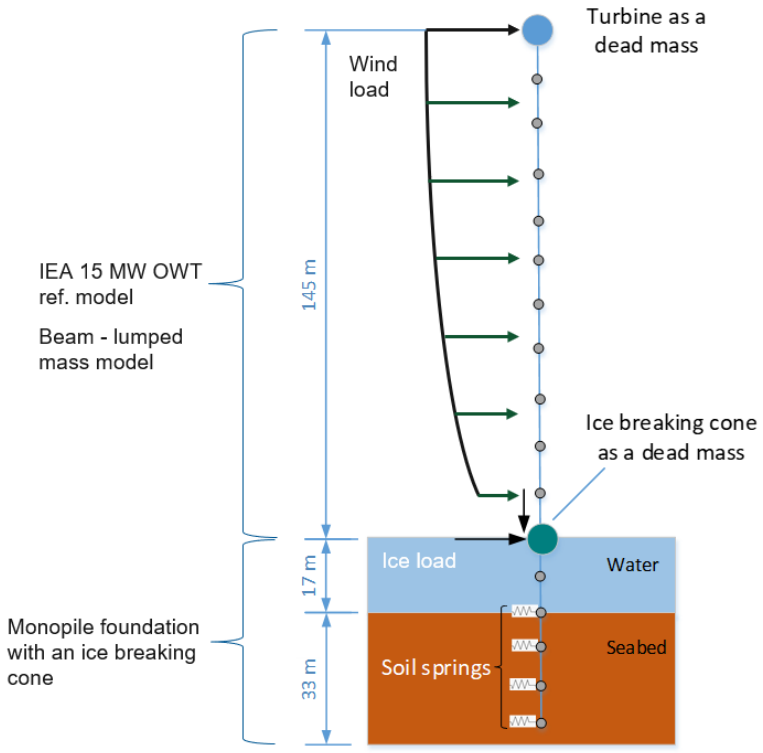

Figure 2. Structural model and the applied loads.

Ice and wind loads

Ice thicknesses are extracted from FMI ice map data from winters 1980/81-2021/22 (Tikanmäki et al. 2025). The used values are average ice thickness values given for each polygon in the digital ice charts (2006/07 onwards). Before that, the average ice thickness was not reported separately. Thus, for earlier years, the average ice thickness is calculated by taking mean from the minimum and maximum ice thickness rounded to the nearest 5cm. The used wind speed data is ERA5 data (2023) from January to April in the years 1981-2023 at a location near Kiisla. Wind shear law is used to determine the wind speed at different heights. The used wind shear factor α_{shear} is 0.14 based on analysis of the used ERA5 data and corresponding to IEC standard (2019). Ice drift speed and direction are determined from wind speed 10 m above water level. Ice drift speed is calculated as 2% or 3% of wind speed at 10 m height. Ice drift direction is assumed to be 0° or 30° right from the wind direction. Ice is assumed to drift when it is not labelled as fast ice in the ice charts. The data is divided into bins with intervals of 0.1 m for ice thickness, 2.5 m/s for wind speed and 45° for wind direction. The wind and ice thickness data are treated as independent variables, where joint occurrence of ice thickness and wind conditions is determined by multiplying the occurrence of individual conditions.

Turbine thrust load history is based on turbine thrust

$$F_{hub} = 0.5\rho A {v_{hub}}^2 C_t \tag{1}$$

with normal turbulence model, where ρ is air density, A is rotor disk area, v_{hub} is wind speed at hub height and C_t is thrust coefficient with values corresponding to the IEA 15 MW reference turbine (Gaertner et al., 2020). The distributed tower load history is based on tower load

$$F_{tower} = 0.61 {v_z}^2 C_h C_s D_{tower} \tag{2}$$

using the same turbulence time history as the turbine thrust load. v_z is wind speed at height z, C_h is height coefficient (1.58), C_s is shape coefficient (0.5) and D_{tower} is tower diameter.

The ice load calculation is according to Jussila and Heinonen (2012). The interaction between the ice breaking cone and the moving ice field is divided into three phases: loading, unloading and gap phases. At the loading phase the cone interacts with the moving ice field causing an increase in the horizontal and vertical force. Maximum horizontal R_H and vertical R_V ice loads are calculated according to the model by Croasdale (2016). The peak value of the horizontal and vertical ice load in each loading phase is considered normally distributed. The mean value of the horizontal and vertical ice load are

$$\begin{aligned} \bar{R}_H &= \frac{R_H}{1+3c}, \\ \bar{R}_V &= \frac{R_V}{1+3c} \end{aligned} \tag{3}$$

where c is coefficient of the standard deviation equal to 0.29. Due to bending failure of the ice field, the horizontal and the vertical forces decrease to zero in the unloading phase. In the gap phase, the cone and the moving ice field do not interact, hence the horizontal and the vertical forces are assumed to be close to zero. Time interval T of adjacent loading phases is defined by ice velocity v and breaking length L_b, which is also considered to be normally distributed:

$$T = \frac{L_b}{v} \tag{4}$$

Fatigue damage estimation

Fatigue damage D is calculated for 25 winters according to IIW Recommendations for fatigue design (2016):

$$D = \sum \frac{n_i}{N_i} \ , \tag{5}$$

where n_i is number of cycles corresponding to stress range $\Delta\sigma_i$ and N_i is number of cycles to failure corresponding to the same stress range. Damage sum of 1 to failure is used. N_i is calculated from S-N curves based on characteristic fatigue resistance (FAT) at 2 million cycles (N_{FAT})

$$N_i = N_{FAT} \left(\frac{FAT}{\Delta\sigma_i}\right)^m \tag{6}$$

For a butt weld with loading direction parallel to the welding direction and under variable amplitude loading, fatigue resistance FAT 125 and slopes $m_1 = 3$ (above FAT curve knee point) and $m_2 = 5$ (below FAT curve knee point) are used. Thickness correction for wall thicknesses above 25 mm is applied with a thickness reduction factor $f_t = (t_{ref}/t)^n$, where t is wall thickness, t_{ref} is reference wall thickness of 25 mm and n is correction exponent with value $n = 0.1$. The number of cycles and corresponding stress ranges are calculated from the simulated 10-minute time histories using Rainflow counting.

RESULTS

Loads and stresses

Figure 3 shows the input ice and wind loads for a scenario with 70 cm thick ice drifting with speed 0.3 m/s, and with ice drift speed assumed to be 2% of wind speed. In this case, the ice and rotor thrust loads are of the same order. Figure 3 shows the three phases of the ice loads in comparison to the continuous wind load history. Ice loads increase from around 380 kN for 10 cm ice to almost 4 500 kN for 90 cm ice. Ice drift speed has little effect on the ice load magnitude, but the number of load peaks increases with increasing speed and decreases with increasing ice thickness. Horizontal ice loads are more than double the vertical ice loads. Rotor thrust varies between around 900 kN to just below 4 000 kN. Highest rotor thrust is at 10.9 m/s wind speed. Tower loads are low compared to the ice and rotor thrust loads.

Based on the vertical von Mises stress distribution in the foundation shown in Figure 4, the cross-section 7.5 m below waterline is chosen for the fatigue damage analysis as a critical location for fatigue. For the different scenarios, the maximum stress range ranges from around 25 MPa to 250 MPa with highest stresses corresponding to highest rotor thrust load at 10.9 m/s wind speed at hub height.

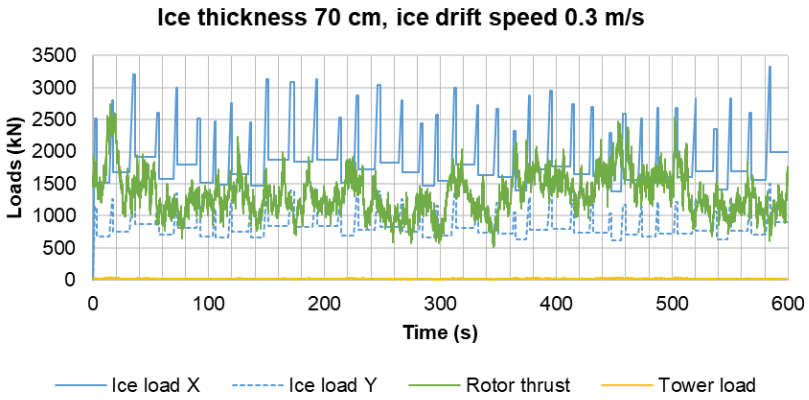

Figure 3. Ice and wind load histories for ice thickness 70 cm and ice drift speed 0.3 m/s. Ice drift speed is 2% of wind speed at 10 m. Wind speed at hub height is 21.8 m/s.

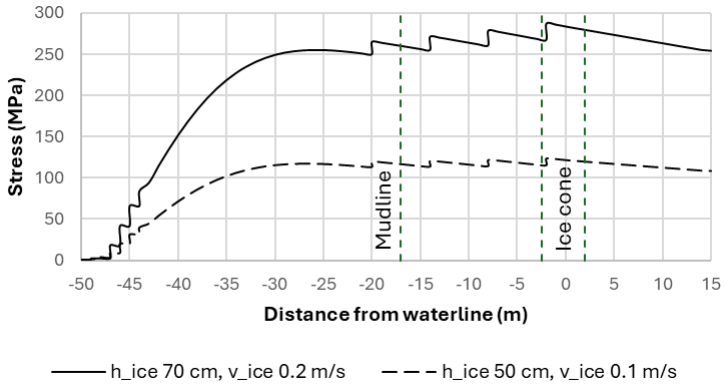

Figure 4. Stress distributions in the foundation for two different ice condition scenarios at the time of maximum peak stress in the simulation. Discontinuities in the curve are due to discontinuity in wall thickness.

Ice conditions and fatigue damage

Table 1 shows an example of the share of different ice thickness and wind speed combinations over the 42-year period from 1981-2022 for months January-April in Kiisla. Wind directions between South and West are included here with wind coming from these directions 33% of the time. These are also the directions with the highest wind speeds. Here, the ice speed is 2% of wind speed at 10 m. Wind speeds above the 25 m/s threshold, when turbine is not operational, account for only 0.1% of the ice season time.

In Table 1, the most often occurring conditions, occurring roughly for one day a year, are highlighted in red. These conditions include hub height wind speeds up to 14.5 m/s (ice drift speed up to 0.2 m/s) and ice thickness up to 60 cm. The most often occurring conditions are wind speeds 3.6 – 10.9 m/s, ice drift speeds 0.05 – 0.15 m/s and ice thicknesses 30 – 50 cm. These account for 6% of the ice season time when ice is drifting (fast ice scenarios are not included in the table). The observed ice thicknesses are up to 90 cm, whereas the hub height wind speed is up to 32.7 m/s and assumed ice drift speed is up to 0.45 m/s.

Table 2 shows the share of calculated fatigue damage for 25 years of ice seasons for the conditions in Table 1. The percentage of time at different conditions directly affects the lifetime number of cycles and therefore the accumulated fatigue damage. For the 10-minute time histories the number of load cycles varies from ranges from 85-150 cycles when the turbine is operational to 130-330 cycles when the turbine is idle. During idling, the stress ranges are lower but still significant for fatigue. When looking at the lifetime of the structure, the number of cycles for the most often occurring conditions (shown in red in Table 1) is in the order of 500 000 cycles, whereas for the highest ice thicknesses above 70 cm and higher ice drift speeds of above 0.25 m/s (shown in green in Table 1), the number of cycles is in the order of tens of thousands. Therefore, ice thicknesses over 70 cm have little effect on accumulation of fatigue damage compared to other conditions.

Table 1. Example of % of time with different wind/ice drift speeds and ice thicknesses based on 41 years of data. Ice drift speed is 2% of wind speed at 10m. Wind direction South-West.

% time for Jan-Apr		Ice thickness (cm), bin max								
Wind speed, hub height (m/s), bin max	Ice drift speed (m/s), bin max	10	20	30	40	50	60	70	80	90
3.6	0.05	0.37	0.41	0.38	0.42	0.47	0.32	0.14	0.06	0.03
7.3	0.1	1.24	1.39	1.27	1.41	1.57	1.07	0.46	0.20	0.09
10.9	0.15	1.30	1.45	1.33	1.48	1.65	1.13	0.48	0.21	0.09
14.5	0.2	0.94	1.05	0.96	1.07	1.20	0.82	0.35	0.16	0.07
18.2	0.25	0.56	0.63	0.58	0.64	0.71	0.49	0.21	0.09	0.04
21.8	0.3	0.26	0.29	0.27	0.30	0.33	0.23	0.10	0.04	0.02
25.4	0.35	0.07	0.07	0.07	0.08	0.08	0.06	0.02	0.01	0.00
29.1	0.4	0.01	0.02	0.01	0.02	0.02	0.01	0.00	0.00	0.00
32.7	0.45	0.00	0.00	0.00	0.00	0.00	0.00	0.00	0.00	0.00

Table 2. Calculated share of fatigue damage with ice drift speed of 2% of wind speed. Cases analyzed up to 0.35 m/s ice drift speed due to diminishing contribution to damage.

% share of fatigue damage		Ice thickness (cm), bin max								
Wind speed, hub height (m/s), bin max	Ice drift speed (m/s), bin max	10	20	30	40	50	60	70	80	90
3.6	0.05	0	0	0	0	0	0	0	0	0
7.3	0.1	2.5	3.6	2.0	2.3	3.0	2.9	1.1	0.4	0.2
10.9	0.15	8.6	9.1	9.3	10.4	11.4	8.2	4.2	1.3	0
14.5	0.2	1.3	1.5	1.3	1.3	2.6	1.4	0.8	0.4	0.1
18.2	0.25	0.5	0.6	0.5	0.4	0.8	0.7	0.2	0.1	0.1
21.8	0.3	0.7	0.7	0.7	0.8	0.7	0.8	0.3	0.1	0
25.4	0.35	0	0	0	0	0	0	0	0	0

Influence of ice drift speed and direction

Tables 3 and 4 show comparisons of four different scenarios for a typical hub height wind speed of 7.3 m/s:
a) Baseline with ice drift speed 0.1 m/s (2% of wind speed) and wind/ice misalignment 0°
b) Higher ice drift speed of 0.15 m/s (3% of wind speed)
d) Wind/ice misalignment with ice drift direction 30° right from wind direction
d) Ice stationary: ice is immobile with no contact between ice and structure, with wind loads included, simulated loads the same for all ice thicknesses

The effect of ice drift speed on stress range and calculated damage varies from negative to positive but increases with increasing ice thickness. For ice thicknesses below 20 cm, the ice drift speed has little influence on maximum stress range, but for ice thicknesses above 50 cm, the stress state can vary up to 12%. From zero wind/ice misalignment i.e. free drift to 30° misalignment (Coriolis force dominating), the effect on maximum stress range is close to zero or approximately ±5%. Ice loads increase maximum stress range up to 11% when compared to the scenario with no ice drift. When comparing the effects to calculated fatigue damage, the influence is much more pronounced, with ice drift having higher impact for thicker ice and wind/ice misalignment having the highest impact for intermediate ice thicknesses.

Table 3. Effect of assumed ice conditions on calculated maximum stress range compared to baseline maximum stress range (in MPa) with ice drift speed 0.1 m/s (2% of wind speed) and wind/ice misalignment 0°.

% change in maximum stress range from load history	Ice thickness (cm), bin max								
	10	20	30	40	50	60	70	80	90
a) Baseline (in MPa)	155	157	145	153	158	167	164	153	151
b) Ice drift speed 3% of wind speed	1%	-1%	6%	2%	-5%	-13%	-11%	12%	11%
c) Wind/ice misalignment 30°	0%	0%	4%	1%	-1%	-4%	-2%	1%	5%
d) Stationary ice	-4%	-5%	3%	-3%	-6%	-11%	-9%	-3%	-2%

Table 4. Effect of assumed ice conditions on calculated fatigue damage compared to baseline case fatigue damage (in %) with ice drift speed 0.1 m/s (2% of wind speed) and wind/ice misalignment 0°.

% change in fatigue damage	Ice thickness (cm), bin max								
	10	20	30	40	50	60	70	80	90
a) Baseline (in %)	2.5	3.6	2.0	2.3	3.0	2.9	1.1	0.4	0.2
b) Ice drift speed 3% of wind speed	4%	-14%	29%	22%	1%	-34%	-46%	54%	31%
c) Wind/ice misalignment 30°	4%	-8%	18%	15%	6%	-10%	-4%	5%	5%
d) Stationary ice	Not comparable								

DISCUSSION

Tables 1 and 2 show that as expected, the share of expected fatigue damage is highest for the lower wind speed / ice thickness combinations, where the number of events is highest. The stress state does not always increase with increasing wind speed and ice thickness as would be expected (see Baseline maximum stress ranges in Table 3). This results from the differences in the timing of wind and ice load peaks, as the location of ice load peaks changes with both changing ice thickness and ice drift speed, whereas the location of wind load peaks changes only for the different ice drift speed scenarios. The likelihood of wind and ice load peaks matching needs to be considered in design analysis. Typically, a stochastic approach is used by applying e.g. 5 versions of a load history. Regarding the ice load model itself, previous research by El Gharamti and Heinonen (2024) has shown that the rubble pile profile is crucial in the modelling process.

Assuming higher ice drift speed of 3% of wind speed resulted in ±12% difference in maximum stress ranges and -46% - +54% difference in damage when compared to baseline ice speed of 0.1 m/s at 2% of wind speed. The high variation is attributed to the fact that the number of ice load peaks during a 10-minute simulation is relatively low and while the wind load history remained the same, the temporal location of the ice load peaks changed leading to different combined wind/ice peak loads. Similar variation is observed for the effect of wind/ice misalignment, but the effect on both the stress state and fatigue damage is smaller.

The calculated influence of ice drifting vs not drifting was up to 11%. In Kiisla area, the average number of ice days during an ice season is 144 days, which is 39% of the year. Of these 144 days, 12 days on average have been labelled as days with fast ice giving an assumed drift percentage of 91.9%. This is a conservative upper bound estimate as ice marked as drift ice does not always drift. Recent measurements in the Bothnian Bay together with the campaign at Norströmsgrund indicate that the actual drift percentage could be 60% or less. This percentage is on average for all ice thicknesses. However, as thicker ice is less likely to drift, the drift ice percentage could be even less for higher ice thicknesses i.e. the higher ice load scenarios.

To account for the fatigue damage from the ice-free season and the probability of ice and wind load peak matching, future work includes the addition of wave loads to the analysis and a stochastic approach in applying the environmental loads. In addition, a more detailed analysis of the load directions, including the now omitted wind directions, is needed to get the full picture of damage accumulation.

CONCLUSIONS

Effect of severe ice conditions on fatigue damage accumulation in offshore wind turbine foundation fitted with an ice breaking cone was estimated. A matrix of ice conditions was compiled from historical ice chart and reanalysed ERA5 data. The effects of ice loads in addition to wind loads with varying drift speeds and directions were simulated for the IEA 15 MW reference wind turbine. A cross-section 7.5 m below waterline was chosen for the fatigue damage calculation.

The most often occurring ice conditions were also the most damaging ones with the exception that ice drift speeds below 0.05 m/s did not contribute to fatigue damage. Fatigue damage from ice events (not including fatigue damage during open water periods) could be increased by as

much as 54% when higher drift speed is assumed (from 2% of wind speed to 3%) and up to 18% because of increase in wind/ice direction misalignment (from 0° to 30°). Significance of results: 1) The most often occurring ice conditions are also the most damaging ones, except for ice drift speeds 0.05 m/s and below. 2) Ice drift speed affects the maximum stress level more than ice/wind misalignment. To deal with the uncertainty arising from the probability of ice and wind load peaks, a stochastic approach for the input load histories is needed as future work.

ACKNOWLEDGEMENTS

The authors gratefully acknowledge the following funders: Terramare-Boskalis, Labkotec Oy, Skarta Energy Oy, Skyborn Renewables AB, OX2, Metsähallitus and Aker Arctic for funding the SBP-IceWind project,the Academy of Finland for funding the WindySea project (Special RRF funding for research on key areas of green and digital transition [grant number 348588]) and RePower project funded by the European Union NextGenerationEU. RePower project is part of the strategic research opening "Electric Storage" of VTT, launched with the support of the additional chapter of the RePowerEU investment and reform programme for sustainable growth in Finland. . Finally, the authors would like to acknowledge Ponvia (currently part of A-Insinöörit) for providing the seabed properties.

REFERENCES

Braun, M., Dörner, A., ter Veer, K. F., Willems, T., Seidel, M., Hendrikse, H., Høyland, K. V., Fischer, C., & Ehlers, S. (2022). Development of Combined Load Spectra for Offshore Structures Subjected to Wind, Wave, and Ice Loading. *Energies*, *15*(2), 559.

Copernicus Climate Change Service, Climate Data Store, 2023: ERA5 *hourly data on single levels from 1940 to present*. *Copernicus Climate Change Service (C3S) Climate Data Store (CDS)*. [Online] Available at: 10.24381/cds.adbb2d47 [Accessed on 7 February 2025].

Croasdale K., Brown T., Wong C., Shrestha N., Li G., Spring W., Fuglem M. & Thijssen J., 2016, Improved equations for the actions of thick level ice on sloping platforms. In OTC Arctic Technology Conference (pp. OTC-27385). OTC.

DNVGL-ST-0437, 2016. *Loads and site conditions for wind turbines*, DNV GL.

El Gharamti I., Heinonen J., 2024. *Parametric study of ice loads on conical structures using the Croasdale model*. 27th IAHR International Symposium on Ice.

Eurokoodin soveltamisohje, 2017. *Geotekninen suunnittelu – NCCI 7. Siltojen ja pohjarakenteiden suunnitteluohjeet*, Helsinki: Liikennevirasto. In Finnish.

Gaertner, E., et al., 2020. *Definition of the IEA 15-Megawatt Offshore Reference Wind.* [Online] Available at: https://www.nrel.gov/docs/fy20osti/75698.pdf [Accessed 5 February 2025].

Hornnes, V., Hammer, T. C., Høyland, K. V., Hendrikse, H. & Turner, J., 2022. *On the use of drift ice thickness statistics from a Copernicus reanalysis product for fatigue damage calculation*, 26th IAHR International Symposium on Ice, pp.

IEC 61400-3-1, 2019. *Wind energy generation systems – Part 3-1: Design requirements for fixed offshore wind turbines*, Geneva: IEC.

IIW, 2016. *Fatigue Design of Welded Joints and Components: Recommendations of IIW Joint Working Group XIII–XV,* IIW/Springer.

Jussila, V. & Heinonen J., 2012. Comparison of Ice-induced Vibrations on a Conical and a Cylindrical Offshore Wind Turbine Substructure. In: Li, Z. and Lu, P., eds., Ice Research for a Sustainable Environment, *21st IAHR International Symposium on Ice*, pp.998-1013

Leppäranta, M., (2011). *The Drift of Sea Ice*. Springer-Verlag:Berlin.

Sinsabvarodom, C., Chai, W., Leira, B. J., Høyland, K. V. & Næss, A., 2022. Ice rose diagrams for probabilistic characterization of the ice drift behavior in the Beaufort Sea. *Ocean Engineering*, 266(2).

Tikanmäki, M., Heinonen, J., Jokiniemi, A., Eriksson, P. B., 2025. Design sea ice conditions for offshore wind power in the Baltic Sea. *Cold Regions Science and Technology*, 234.

Tikanmäki, M. Heinonen, J., 2021. Estimating extreme level ice and ridge thickness for offshore wind turbine design: Case study Kriegers Flak. *Wind Energy*, 25(4).